International Journal of Engineering Innovation & Research
Volume 6, Issue 2, ISSN: 2277 – 5668

# Densely Packed Vertically Aligned Carbon Nanotube-Polymer Composite Membrane Fabrication and Characterization for Selective Filtration of Liquids

**Samarth Trivedi***
*email id: sam2025in@gmail.com

**Kamal Alameh**
email id: k.alameh@ecu.edu.au

Electron Science Research Institute, Edith Cowan University, 270 Joondalup Drive, Joondalup, WA 6027, Australia
*Corresponding author

*Date of publication (dd/mm/yyyy): 24/04/2017*

***Abstract* — In this paper, the permeance of membranes based on the use of high-density Vertically-Aligned Carbon Nanotubes (VACNTs) in conjunction with Polydimethylsiloxane (PDMS), as filler material, are investigated for polar and non-polar liquids. Reactive ion etching is used to enhance the hydrodynamic flow properties of the VACNT membranes. Experimental results show that RIE treatment introduces hydroxyl ions (-OH) on the surface of the VACNT membranes, thus enhancing their gatekeeping activity and hydrophilicity simultaneously, and leading to an increase in flow rate for polar and non-polar liquids. The measured permeance improvement factors for water, ethanol, IPA, hexane and gasoline are 100%, 37.2%, 11.8%, 20.9% and 3.8%, respectively, with respect to Oxygen-plasma-treated VACNT membranes.**

***Keywords* — Polar and Non-Polar Liquid Filtration, Nano-Membranes, Vertically Aligned Carbon Nanotubes.**

## I. INTRODUCTION

Vertically-Aligned Carbon Nanotube (VACNT) membranes mimic natural protein channels in terms of (1) enhancing fluid flow, (2) acting as a chemical "gatekeeper" at the entrance and (3) enabling electrochemical transformations through their electrical conductivity. These properties of VACNT membranes make them attractive for applications in medical science, such as drug delivery, in environmental science, such as water filtration and sensing. Many factors typically affect the molecular or ionic transport properties of VACNTs, including the diameter of the channel, the size of molecule, the hydrodynamics of the channel, and the ion capping selectivity at the channel entrance. Over the last decade, some artificial protein channel structures have been mimicked using two classes of materials, namely, (i) metals, such asAnodized Aluminium Oxide (AAO), and (ii) pristine carbon structures, such as VACNTs. The greatest challenge associated with such structures is that the gatekeeper at the entrance of the channel reduces the fluid flow and has a limited chemical selectivity. However, protein channels still support very fast water molecule transport, and hence, VACNT based membranes are anticipated to provided superfast transport of water molecule through their channels.

High molecule velocities due to frictionless surface inside CNTs have been experimentally observed [1, 2]. Majumdar et al. [3] have demonstrated fast interfacial "slip velocity" in the pore walls of CNTs due to their large non-interacting van-der-Waals length and atomically-flat surface, which would not scatter the flowing fluid. The chemistry of such phenomenon can be explained by Molecular Dynamic (MD) simulation, which predicts the H-bond coupling of water molecule with the internal surface of the CNT walls [4]. Recently, superfast transport of liquid and gases across CNT-based membraneshas been demonstrated [5 – 12].

This paper discusses the use of Reactive Ion Etching (RIE) to enhance the hydrodynamic flow properties of the densely-packed highly-ordered VACNTs with 5nminner diameter, and experimentally investigates the performance of the developed membranes for the filtration of polar and non-polar liquids. Experimental results demonstrate the ability of RIE treatment to enhance the gatekeeping activity and hydrophilicity of the developed VACNT membranes, simultaneously, thus leading to increase in the flow rate of water, ethanol, IPA, hexane and gasoline by 100%, 37.2%, 11.8%, 20.9% and 3.8%, respectively, in comparison with Oxygen-plasma-treated VACNT membranes.

## II. EXPERIMENTAL METHOD

Several high-density VACNT samplesofCNT inner and outer diameters 5nm and 8 nm, respectively, and length 300 µm, were specially developed by DK NanoMaterials Co. Ltd (China) using chemical Vapour Deposition (CVD). The VACNTs were developed by DK Nanomaterials Co. Ltd. (China) confirmed the density, diameter of CNT, tortuosity, vertical alignment and pristine quality of grown VACNTs using Transmission electron microscopy (TEM), Scanning electron microscopy (SEM) and Thermogravimetric analysis (TGA). Fig. 1 shows a cross-section of one of the developed VACNT array, which was obtained using a ZEISS-NEON 40ESP FIB/SEM system in conjunction with a stage of variable tilting angle.SEM images captured using an FIB-SEM (Focussed ion beam scanning electron microscope, Zeiss - Neon 40 EsB), confirmed the high density ($10^{11}$ CNT/cm$^2$) of the developed VACNTs. The VACNTs were grown onto a silicon wafer, which was glued onto a glass substrate, purely for mechanical support, and placed in a spin coater, where 50% (w/w) PDMS mixed with Xylene was added drop by drop. The samples were spin-coated at a speed of 2500 rpm, and thendried in a vacuum oven for 6 hours. Subsequently, each sample was detached from the glass substrate and then sliced into 25 µm thick membranes using a microtome machine, as illustrated in Fig. 2.

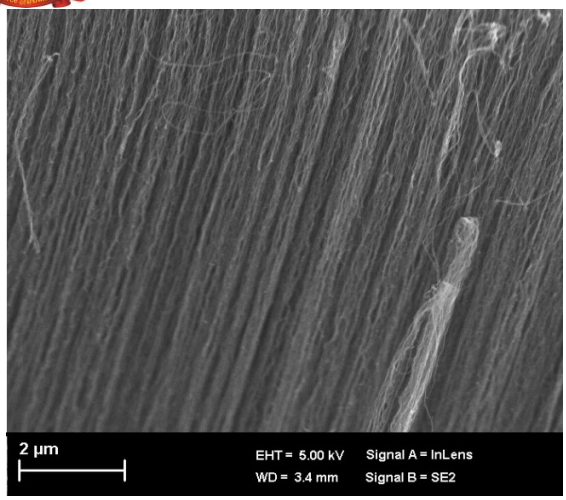


**Figure 1.** Cross section of the developed VACNT array.

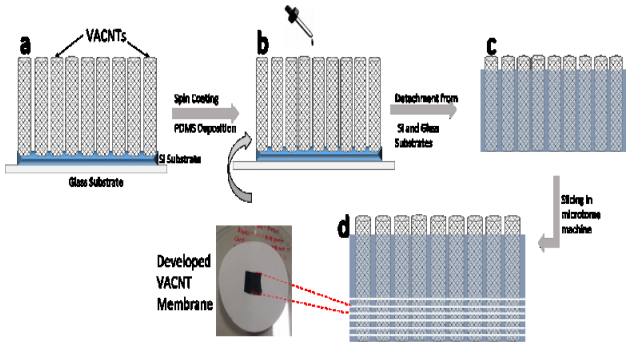


**Figure 2.** VACNT membrane fabrication process. a) VACNT on silicon substrate glued to glass. b) PDMS addition and spin coating. c) After drying, silicon and glass substrates are detached using mechanical peeling. d) VACNT-PDMS composite is sliced using a microtome machine [14].

The 25 µm thick membrane ofVACNT-PDMS mix matrix was treatedwithreactive ion etching (RIE) at a vacuum pressure of 150 mTorr for 45 seconds, 37:13 sccm of $CF_4$ : $O_2$ gases and an RF power was 150 W. Each RIE treated sample was transferred onto a porous Polyvinylidene fluoride (PVDF) support membrane, which was mainly used as a backbone to provide additional mechanical support to the VACNT-PDMS mix matrix membrane. Note that, the PVDF support membrane had no contribution to the active filtration process.

Every etched membrane was then installed in a crossflow cell,shown in Fig. 3, where the membrane was placed on a wire mesh support and sandwiched between acrylic plates before sealing the cell with O-rings, thus forcing the liquid feed to pass through the membrane at high pressure.

Note that, during the fabrication process, open ends of the VACNTs were exposed to the highly-viscous polymer, however, subsequently the VACNT-PDMS block was sliced using a microtome machine, which eliminates possibility of CNT ends being blocked by the polymer material. Additionally, the RIE treatment, after slicing, ensured the removal of any unexpected blockage, and this was also confirmed by a pressure test.

Fig. 4 shows the experimental setup that was used to investigate the performance of the developed VACNT membranes. For liquid filtration, a stock solution was pumped to the cross flow cell via a peristaltic pump at a pressure that was controlled by a pressure gauge. The unfiltered feed was then sent back to the stock-solution tank and mixed with it. Permeate was collected by the permeate tank and its quality was analysed.

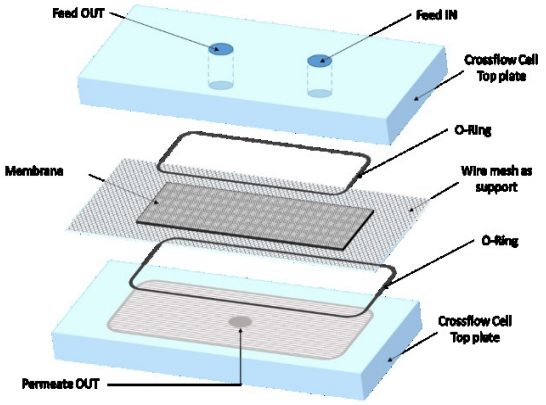


**Figure 3.** Schematic of the developed crossflow cell. The VACNT membrane is placed on a wire mesh support and sandwiched between acrylic plates before sealing the cell with O-rings to enable feed filtration at high pressure.

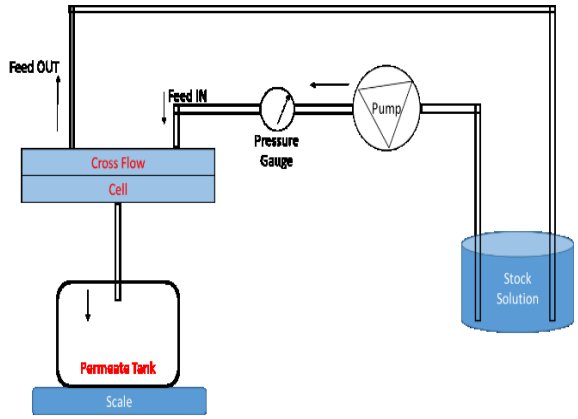


**Figure 4.** Benchtop crossflow setup used to investigate the performance of the developed VACNT membranes.

Note that, the feed was continuously circulated via the peristaltic pump to keep the feed concentration uniform throughout the experiment.

Experiments were performed using the dead-end filtration setup shown in the fig. 5 below, where feed flow through the membrane is forced using a vacuum pump rather than direct pressure [13]. The dead end cell used in the experiments comprised a bottom collection chamber with a magnetic stirrer, a ceramic support onto which the VACNT membrane was placed, a polyurethane gasket (sealer) that prevented water/gas leakage through the membrane edges and a water reservoir. The VACNT membrane was fed from a water reservoir containing water of salinity initial 10,000 ppm, and a vacuum pump was used to create pressure gradient that enables water to flow through the membrane. During the experiments, negative pressure was applied to the modified dead-end cell setup, with an ambient pressure of 780 torr applied at the feed side and vacuum of 640 torr at collection side. The vacuum pressure

at the permeate side was monitored by a pressure gauge and the quality of permeate was monitored using a salinity sensor. As vacuum was applied to the permeate-collecting container, the solution was automatically degassed, and this degassed solution was used to measure the water flux. The volume of the collected permeate was recorded every minute for 60 minutes. Note that, as illustrated in the below figure, a decrease in flux with time was experienced since the feed was not stirred.

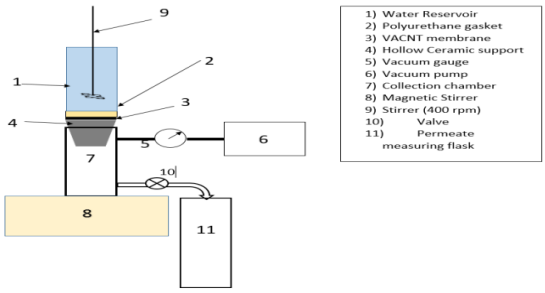


**Figure 5.** Modified dead-end cell setup used to measure the VACNT membrane performance [14].

Prior to the experiment, the benchtop crossflow setup, the modified dead-end cellandthe prepared membranes were checked up for cracks or leakage through the cell's edges at 2 bars and 4 bars. A50 ppm $Fe_2O_3$ solution of 10 nm particle size was used to test the filtration capability of the 25 µm thick membranes at high pressure. Fig.6 shows the measured UV-Vis spectra of the iron oxide solution at the feed side and the collected permeate. It is obvious from Fig. 6 that the absorption of the collected permeate is significantly reduced after filtration, confirming the ability of the VACNT membranes to produce clear and colourless permeate water.

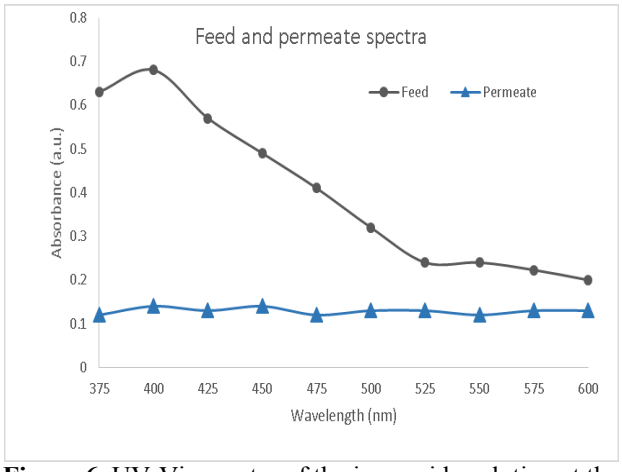


**Figure 6.** UV-Vis spectra of the iron oxide solution at the feed side and the collected permeate [14].

The permeate flux of various liquid was measured at the standard conditions for the evaluation of 20° C and at 2 bar. The pure water flux was then calculated using the followingequation [15]

$$Q = \frac{M}{A\Delta t} \quad (1)$$

Where M is the weight of permeate water (Kg). A is the membrane area ($m^2$), Δt is the permeation time (h)

The liquid flow through porous membrane was calculated using Hagen-Poiseuille equation [15]

$$J = \frac{\varepsilon_p \mu r^2 \Delta p}{8\mu\tau L} \quad (2)$$

where $J$ is the flow of liquid, $\varepsilon_p$ is the relative porosity, $r$ is pore radius, $P$ is the pressure applied, $\mu$ is the dynamic viscosity, τ is the tortuosity (1.1) and $L$ is the length of the pore.

## III. Result and Discussion

The prepared samples were tested for salt rejection capability using the modified dead-end cell setup, shown in Fig. 6, over a time period of 60 min. Fig. 7 shows the salt rejection versus time for the various developed VACNT membranes. The salinity of the feed was 10,000 ppm NaCl solution and the salinity of the collected permeate was continuously monitored using a Vernier salinity probe at a time interval of one minute [12-17]. The salt rejection was simply calculated using the following equation [18]

$$R(\%) = \left(1 - \frac{C_p}{C_f}\right) \times 100 \quad (3)$$

Two main factors typically affect the salt ion rejection, namely, 1) diameter of the carbon nanotubes and 2) the surface charge of the material used to fabricate the membrane. Note that the negatively-charged native PDMS surface traps $Na^+$ ions [19], thus increasing the salt rejection of the PDMS-CNT membrane. During the experiments, initially, the surface charge of the membrane was high, since both the low CNT diameter and high surface charge of the membrane contributed to the high salt rejection of the membrane.The salt rejection was decreased to 97% from 99% in first 10 mins due to concentration polarization but after 10 mins the salt rejection stabilized at 97% and it was constant for remaining time period. After 60 minutes of filtration, concentration polarization reduced the salt rejection contributed by the surface charge of the membrane, as evident from Fig. 7, wherein the experimental results are in agreement with the results reported by Schrott et al. [20].

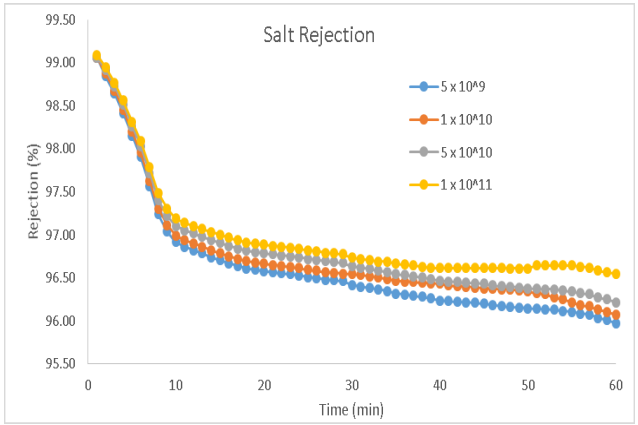


**Figure 7.** This is extracted graph of the Salt rejection versus time, for the different developed VACNT membranes [14].

Note that, the iron oxide particles were used only to show size exclusion, and Fig. 6 shows the UV-Vis absorbance spectra of the iron oxide particles in feed and permeate solutions. Note also that, the increase in NaCl rejection with increasing the hole size can be attributed to (i) the fact that salt rejection decreases with increasing the CNT diameter [21] and (ii) the negatively charged CNT surface traps $Na^+$ ions [21], and hence, reduces salt passing through large holes.

The increase in flux is not directly proportional to the VACNT density. This is because when the density of VACNT increases, the number of CNT walls also increases, while the active inner diameter of CNT remains the same. Therefore, the slight increase in flow rate is attributed to additional small volumes of water flowing between walls of the MWCNTs.

The permeance of the prepared VACNT membranes were analysed for various polar and non-polar liquids. Inspired by the selective ionic transport capability of protein channels RIE etching was a proposed and investigated as an effective process for opening the VACNT pores and making the membrane surface smoother. In addition, the RIE process not only opened the VACNT pores but also changed the electrochemical properties of the VACNTs and PDMS at the surface of the membrane through the introduction of active hydroxyl ion[22], as illustrated in Fig.8(a).

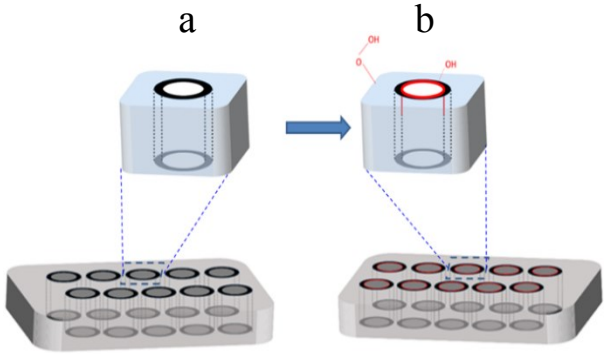


**Figure 8.** a) Hole opening after dry etching (RIE). b) Illustration of the formation of hydroxyl ion on PDMS and VACNT entrance. The black rings represent MWCNTs, whereas the dotted line connecting the black rings between the top to bottom surfaces of the membrane are just a depiction of the vertical alignment of the CNTS.

Fig.8. (a) Hole opening after dry etching (RIE). (b) Illustration of the formation of hydroxyl ion on PDMS and VACNT entrance. The black rings represent MWCNTs, whereas the dotted line connecting the black rings between the top to bottom surfaces of the membrane are just a depiction of the vertical alignment of the CNTs.

As illustrated in Fig. 8 (b), hydroxyl ions are introduced only at the entrance of the VACNT membrane, since plasma etching mainly reacts with the surface of the membrane, thus adding two major functions, namely (i) selective ionic transportation of liquid with different molecular size and (ii) selective permeation[23]. Note that, other factors might also affect the selective permeation feature, such as the ionic strength of liquid, the functional groups present in the liquid and its chain length.

Another feature was developed by the dry etching, that is, the membranes became more hydrophilic, instead of being hydrophobic. This feature was demonstrated through surface tension measurements. As illustrated in Fig.9, which shows a change in contact angle formed by a water drop on the VACNT membrane before and after RIE etching. The change in contact angle from 60° to 42° after etching, confirms the change of the hydrophobicity of the RIE-treated VACNT membrane and reveals the presence of hydroxyl ions on the VACNT entrances, as reported by Majumdar et al. [3].

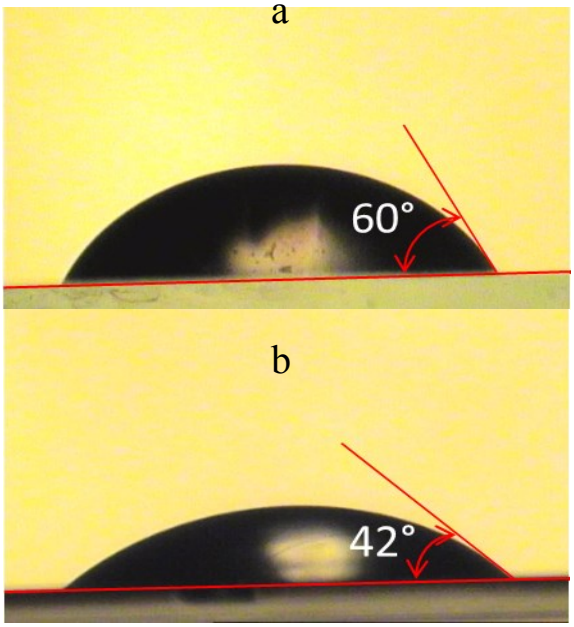


Figure 9. Photographs of a water drop on the VACNT membrane a) before RIE etching and b) after RIE etching. Contact angle decreases from 60° before etching to 42° after etching.

Table 1 shows the permeance of the developed VACNT membranes for various liquids that were filtered through, before and after RIE treatment. Also shown in Table 1 is the permeance of VACNT membranes for various liquids, those were etched using oxygen plasma [3].

**Table 1.** Permeance of the 25 µm-thick VACNT membranes for various liquids, before and after RIE treatment. Average inner CNT diameter: 5 nm, CNT density: $1 \times 10^{11}$ $cm^{-2}$.

| Liquid | Viscosity (cP) | Permeance before etching (LMHBar) | Permeance after etching (LMHBar) | Permeance of reported etched VACNT membrane (LMHBar) [3]* | Improvement factor (%) |
|---|---|---|---|---|---|
| Water | 1.0 | 1203 | 1202 | 600 | 100 |
| Ethanol | 1.1 | 330 | 288 | 210 | 37.2 |
| Isopropyl alcohol | 2.0 | 64 | 59 | 52.8 | 11.8 |
| Hexane | 0.3 | 307 | 319 | 264 | 20.9 |
| Gasoline | 0.3 | 33 | 33 | 31.8 | 3.8 |

*VACNT density used in experiments was $3.4 \times 10^9$ $cm^{-2}$

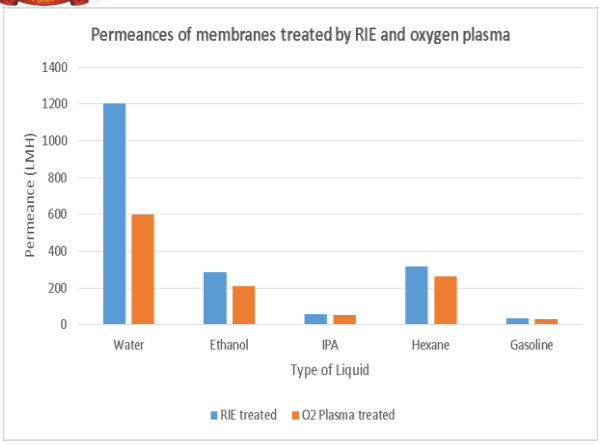


**Figure 10.** Permeance of RIE-treated PDMS-based (blue bars) and Oxygen-plasma-treated Polystyrene-based (orange bars) VACNT membranes, for various polar and non-polar liquids.

Fig.10(data extracted from Table 1) shows the permeance of the RIE-treated PDMS-based (Blue bars) and Oxygen-plasma-treated Polystyrene-based PDMS-based (orange bars) VACNT membranes, for various liquids. The measured improvement factors in permeance for water, ethanol, IPA, hexane and gasoline are 100%, 37.2%, 11.8%, 20.9% and 3.8%, respectively.

Note that oxygen plasma treatment typically introduces carboxylic group (-COOH) on the surface of a VACNT membrane, thus improving its gatekeeping activity without affecting its hydrophobicity[22]. On the other hand, RIE treatment introduces hydroxyl group (-OH) on the surface of the VACNT membrane, thus simultaneously introducing gatekeeping activity and improving the membrane's hydrophilicity (hence, increasing its permeance for water). The –OH bondsof water moleculesinteracts with the walls of the VACNTsto form depletion layerswith a reduced number of hydrogen bonds, thus enhancing the flow rate by reducing friction [7]. Note, on the other hand,that ethanol also has one–OH bond, however, its effect is weak, and therefore,the flow rate for ethanol is comparativelyless than that of water[23].

Typically, the hydrogen bondsof water are not the only factor that affects the flow ratethrough RIE-treated VACNT membranes. The size of the liquid molecules is also an important factor that controls the flow rate through VACNT membranes[24]. Finally, it is important to note that thecontribution of electrostatic interactions between fixed membrane charges and mobile ions to the ion rejection capability of etched VACNT membranes are much more significant than that of the steric and hydrodynamic effects[25].

Finally, it is important to mention that high-resolution SEM and TEM images were used to measure the tortuosity of the VACNT membrane transport channels, which was 1.2.

## IV. Conclusion

Highly-dense RIE-treated VACNT–PDMS membranes have been developed and their permeance have experimentally been investigated forpolar and non-polar liquids. Experimental results have shown that the permeance of the developed VACNT membranes is enhanced by the negatively-charged hydroxyl ionsintroduced into the entrance of the VACNTs by the RIE etching process. Experimental results have also shown that the permeance of the RIE membrane for water, ethanol, IPA, hexane and gasoline is enhanced by 100%, 37.2%, 11.8%, 20.9% and 3.8%, respectively, in comparison with an oxygen-plasma treated VACNT membrane.

## References

[1] V. P.Sokhan et al.,"Fluid flow in nanopores: Accurate boundary Conditions for carbon nanotubes." in J. Chem. Phys., vol. 117, 2002, pp. 8531-8539

[2] TOhbaet al., "Structures and stability of water nanoclusters in hydrophobic nanospaces." in Nano Lett., vol. 5, 2005, pp. 227-230

[3] MMajumdar et al., "Mass transport through carbo nanotube membranes in three different regimes: Ionic diffusion and gas and liquid flow", in ACS Nano., vol. 5, 2011, pp. 3867-3877

[4] GHummer et al."Water conduction through the hydrophobic channel of a carbon nanotube", in Nature, vol. 414, 2001, pp. 188-190

[5] Lee, B; et al."A carbon nanotube wall membrane for water treatment", in Nature comm., vol. 6, 2015, pp. 7109

[6] Hinds, B. Jet al. "Aligned multiwalled carbon nanotube membranes", in Science, vol. 303, 2004, pp. 62-65

[7] Holt, J. Ket al. "Fast mass transport through sub-2-nanometer carbon nanotubes", in Science, vol. 312, 2006, pp. 1034-1037

[8] Mi, W. Let al. "Vertically aligned carbon nanotube membranes on macroporous alumina supports", in J. Membr. Sci., vol. 304 2007, pp. 1-7

[9] Kim, S et al."Scalable fabrication of carbon nanotube/Polymer nano-composite membranes for high flux gas transport", in Nano Lett., vol. 7, 2007, pp. 2806-2811

[10] Srivastava, A et al."Carbon nanotube filters", in Nat. Mater., vol. 3, 2004, pp. 610-614

[11] Yu, M et al."High density, vertically-aligned carbon nanotube membranes", in Nano Lett., vol. 9, 2009, pp. 225-229

[12] Majumder, M et al."Nano-scale hydrodynamics-Enhanced flow in carbon nanotubes", in Nature, vol. 438, 2005, pp. 44-44

[13] Srivastava, A et al."Carbon nanotube filters"in Nat. Mater., vol. 3, 2004, pp. 610

[14] Trivedi, S et al."Effect of vertically aligned carbon nanotube density on the water flux and salt rejection in desalination membranes", in SpringerPlus, vol. 5, 2016, pp. 1158

[15] Mulder, M. "Basic principles of membrane technology", in Kluwer Academic Publishers: Dordrecht, The Netherlands, 1997

[16] Sears K. "Recent developments in carbon nanotube membranes for water purification and gas separation", in Materials, vol. 3, 2010, pp. 127

[17] Verweij H. "Fast mass transport through carbon nanotube membranes",in Small, vol. 12, 2007, pp. 1996

[18] Michael T. "A computational assessment of the permeability and salt rejection of carbon nanotube membranes and their application to water desalination"in Phil. Trans. R. Soc. A., vol. 374, 2015, pp. 20150020

[19] Ocvirk, G. "Electrokinetic control of fluid flow in native poly(dimethylsiloxane) capillary electrophoresis devices", in Electrophoresis, vol. 21 2000, pp. 107

[20] W. Schrott. "Study on surface properties of PDMS microfluidic chips treated with albumin", inBiomicrofluidics, vol. 3, 2009, pp. 044101

[21] Zhang, L et al."Preparation and transport performances of high-density, aligned carbon nanotube membranes",in Nanoscale Res Lett., vol. 10, 2015, pp. 266

[22] Chen, W et al."Photolithographic surface micromachining of polydimethylsiloxane (PDMS)",in Lab Chip., vol. 12, 2012, pp. 391-395

[23] Du, F et al."Membrane of vertically aligned super long carbon nanotubes",in Langmuir, vol. 27, 2011, pp. 8437-8443
[24] Majumder, M et al."Effect of tip functionalization on transport through vertically oriented carbon nanotube membranes",in J. Am Chem. Soc., vol. 127, 2005, pp. 9062-9070
[25] Fornasiero, F et al."Ion Exclusion by sub-2-nm Carbon Nanotube Pores", in Proc. Natl. Acad. Sci., vol. 105, 2008, pp. 17250–17255

## AUTHOR'S PROFILE

**Samarth Trivedi** received the M. S. degree in Environmental Science from the Sardar Patel University, Gujarat, India. He is currently doing Doctoral degree at Electron Science Research Institute, Edith Cowan University, Western Australia, Australia, Since 2013. He is experience in cleanroom technology, nanofabrication, opto-electronic sensing devices. His research interest Include Nanomaterial, nanotechnology, micro/nano sensors, semiconductors, Environmental science

**Kamal Alameh** received the M.Eng. degree in Photonics from the University of Melbourne, Melbourne, Australia, in 1989, and the Ph.D. degree in Photonics from the University of Sydney, Sydney, Australia, in 1993. He is currently a Professor of MicroPhotonics and Director of the Electron Science Research Institute (ESRI) and the WA Centre of Excellence for MicroPhotonic Systems, Edith Cowan University, Joondalup, Australia. He is also a World-Class University (WCU) Professor with the Department of Nano-bio Materials and Electronics, Gwangju Institute of Science and Technology (GIST), Korea, Adjunct Professor with Glamorgan University, Wales, U.K., and Guest Professor with Southeast University, Nanjing, China. He has pioneered the integration of microelectronic and photonic sciences and developed a new and practical research area, "MicroPhotonics," and currently he is engaged in research and development on Opto-VLSI, optoelectronics, and micro-/nano-photonics targeting innovative solutions to fundamental issues in ICT, agriculture, health, consumer electronics, and security and defense. He has authored or co-authored over 250 peer-reviewed journal and conference papers, including three book chapters, and filed 24 patents.